SCIENTIFIC REPORTS

OPEN

SUBJECT AREAS:

EXPERIMENTAL MODELS OF DISEASE

CHRONIC LYMPHOCYTIC LEUKAEMIA

MACROAUTOPHAGY

DRUG DEVELOPMENT

Received
2 October 2012

Accepted
23 January 2013

Published
14 February 2013

Correspondence and requests for materials should be addressed to S.T. (s.tauro@dundee.ac.uk) or P.J.C. (p.j.coates@dundee.ac.uk)

* These authors contributed equally to this work.

# Dysregulation of autophagy in chronic lymphocytic leukemia with the small-molecule Sirtuin inhibitor Tenovin-6

Stephanie F. MacCallum[1]*, Michael J. Groves[1]*, John James[2], Karen Murray[1], Virginia Appleyard[1], Alan R. Prescott[2], Abed A. Drbal[3], Anna Nicolaou[3], Joan Cunningham[4], Sally Haydock[4], Ian G. Ganley[5], Nicholas J. Westwood[6], Philip J. Coates[1,7], Sonia Lain[1,8] & Sudhir Tauro[1]

[1]Dundee Cancer Centre, Ninewells Hospital, University of Dundee, Dundee, Scotland, United Kingdom DD1 9SY, [2]Cell Signalling and Immunology, College of Life Sciences, University of Dundee, Scotland, United Kingdom DD1 5EH, [3]School of Pharmacy and Centre for Skin Sciences, School of Life Sciences, University of Bradford, Bradford BD7 1DP, UK, [4]Department of Cytogenetics, Ninewells Hospital and Medical School, Dundee, Scotland, United Kingdom DD1 9SY, [5]MRC Protein Phosphorylation Unit, College of Life Sciences, University of Dundee, Scotland, United Kingdom DD1 5EH, [6]School of Chemistry and Biomedical Sciences Research Complex, University of St Andrews and EaStCHEM, St Andrews, Fife, UK, KY16, [7]Tayside Tissue Bank, Ninewells Hospital, University of Dundee, Dundee, Scotland, United Kingdom DD1 9SY, [8]Department of Microbiology, Tumor and Cell Biology, Karolinska Institutet, Nobels väg 16, 171 11 Stockholm, Sweden.

**Tenovin-6 (Tnv-6) is a bioactive small molecule with anti-neoplastic activity. Inhibition of the Sirtuin class of protein deacetylases with activation of p53 function is associated with the pro-apoptotic effects of Tnv-6 in many tumors. Here, we demonstrate that in chronic lymphocytic leukemia (CLL) cells, Tnv-6 causes non-genotoxic cytotoxicity, without adversely affecting human clonogenic hematopoietic progenitors *in vitro*, or murine hematopoiesis. Mechanistically, exposure of CLL cells to Tnv-6 did not induce cellular apoptosis or p53-pathway activity. Transcriptomic profiling identified a gene program influenced by Tnv-6 that included autophagy-lysosomal pathway genes. The dysregulation of autophagy was confirmed by changes in cellular ultrastructure and increases in the autophagy-regulatory proteins LC3 (LC3-II) and p62/Sequestosome. Adding bafilomycin-A1, an autophagy inhibitor to Tnv-6 containing cultures did not cause synergistic accumulation of LC3-II, suggesting inhibition of late-stage autophagy by Tnv-6. Thus, in CLL, the cytotoxic effects of Tnv-6 result from dysregulation of protective autophagy pathways.**

Chemotherapeutic drugs currently used to treat patients with chronic lymphocytic leukemia (CLL) achieve disease control through genotoxic activation of p53-dependent signaling in leukemic cells[1–3]. The importance of p53-pathway activity to clinical responses in CLL patients receiving chemotherapy has been demonstrated both *in vitro* and *in vivo*[1–7]. Outcomes have improved further with the use of immunochemotherapy[8], but treatment-associated hematological toxicity is a significant problem, particularly in the elderly. Resistance to therapy too can be a problem in patients with *TP53* mutations[5–7] or dysfunctional p53-associated signal transduction[4], and in disease progressing after previous nucleoside analogue exposure[7]. Consequently, there is a need to develop non-toxic anti-leukemic agents capable of dysregulating leukemic cell survival through novel mechanisms.

Newer therapeutic strategies against CLL include drugs that do not directly target the cellular genome. There has been interest in the epigenetic targeting of CLL through inhibition of histone deacetylase (HDAC) enzymes[9], known to regulate chromatin remodeling and gene expression[10–12]. Most studies have investigated drugs that inhibit class I, II and IV HDAC enzymes[10,13,14], and the effects of class III HDAC inhibition have only recently been described[15,16]. Class III HDACs, also termed Sirtuins (SirT), are structurally distinct from class I and II HDACs, and are evolutionary conserved NAD(+)-dependent acetyl-lysine deacetylases and ADP ribosyltransferases involved in the tissue-specific control of cellular metabolism and lifespan[17,18]. The ability to prolong lifespan is mediated through stimulation of autophagy, a highly conserved protective process that maintains cellular homeostasis during periods of stress[19,20]. In addition, Sirtuins can regulate cellular proliferation and survival through the deacetylation of a variety of non-histone substrates that regulate cellular development[21,22]. Most notably, Sirtuins act to deacetylate p53, thereby limiting p53-dependent growth arrest and apoptosis, making targeted inhibition of these enzymes potentially therapeutic in neoplasia with wild-type *TP53*.

Consistent with this view, compounds collectively referred to as Tenovins[23], were identified by a small molecule screen for agents that induce p53 activation in tumor cells and were shown to target SirT1 and SirT2 (two of 7 Sirtuin isoforms). Tenovins induce apoptosis in malignant cell lines, including those derived from lympho-reticular neoplasia and decrease human tumor growth in xenograft models[24,25]. In these studies, cell death was associated with inhibition of SirT-induced p53 deacetylation and inactivation, resulting in amplification of p53-dependent responses. Anti-leukaemic properties of Sirtuin inhibitors have also been demonstrated in recent pre-clinical studies on Tenovin in chronic myeloid leukaemia[26,27] and Nicotinamide in CLL[15], in association with increased p53-pathway function. However, Sirtuin antagonists differ in their specificity, binding-properties and relative potencies against target enzymes[28], and therefore, the biological effects of different Sirtuin inhibitors can be unique and tissue-specific. Indeed, cell death in response to treatment with the Sirtuin inhibitors sirtinol, cambinol or EX527 in CLL is associated with p53-independent apoptosis[16] and Tenovin can be cytotoxic even in the presence of mutant *TP53*[24].

Due to this potential for tissue and context-dependent differences in biological responses achieved with Sirtuin inhibitors, we examined the *in vitro* effects of one of the Tenovins, Tenovin-6 (Tnv-6) on primary human CLL cells.

## Results

**SirT1 is expressed in CLL.** Since Tenovins target Sirtuins and can enhance wild-type p53 activity[23–25], we first investigated whether CLL cells express Sirtuins and contain wild-type p53. By Western blotting, SirT1 protein was detectable at approximately 80 kDa in protein extracts from all 10 CLL specimens screened. In some specimens, additional bands were observed, particularly when the exposure-time of the Western Blot was increased (Supplementary Figure 1). However, despite longer exposure times, no band indicative of SirT1 was detectable in normal blood lymphocytes. Our observations thus confirm recent studies on SirT1 expression in CLL[15,34,35], and indicate heterogeneity of protein expression between patients.

Sequencing of exons 5–9 of *TP53* revealed no mutations and there was absence of del(17p) by fluorescence *in situ* hybridization.

**Anti-leukaemic cytotoxicity of Tnv-6 is similar to conventional treatment.** After 24 hours of culture, a dose-dependent cytotoxic effect of Tnv-6 was evident in the MTS assay. The mean metabolic activity from 10 patients (assayed in triplicate) with 10 μM of Tnv-6 (39.7 ± 24.11%) was lower than with 5 μM or 1 μM (71.64 ± 24.05% and 95.76 ± 11.35% respectively; $p = 0.005$, Figure 1) and similar to that with fludarabine (42.84 ± 11.03%). A reduction in metabolic activity with 10 μM Tnv-6 was evident even at 8 hours of incubation (84.16 ± 9.9% of controls, $p = 0.007$), similar to the effects of fludarabine (83.96 ± 6.82%) and therefore, further characterization of the cellular response to Tnv-6 was undertaken predominantly in 8 hour cultures.

**Tnv-6 does not affect normal hematopoiesis.** In contrast to the effects of Tnv-6 on CLL cells, the proportion of HPC recovered following 8 hours of culture with 10 μM Tnv-6 (102 ± 38.8 per $2 \times 10^5$ cultured MNC, $n = 4$) was similar to that in control cultures (99.12 ± 39.5, $n = 4$, $p = 0.5$) (Figure 2). Thus, the dose and duration of exposure to Tnv-6 that induces cytotoxicity in CLL cells does not cause hematopoietic toxicity *in vitro*. In contrast, the HPC yield from cultures containing fludarabine was significantly lower (75.3 ± 26.11, $n = 4$) than in control ($p = 0.017$) or Tenovin-6 containing cultures ($p = 0.021$).

In mice treated with Tnv-6, no differences in the cellularity of blood, marrow or spleen were observed after 7 and 19 days of treatment compared to control animals, indicating the absence of short-term hematopoietic toxicity with Tnv-6[26].

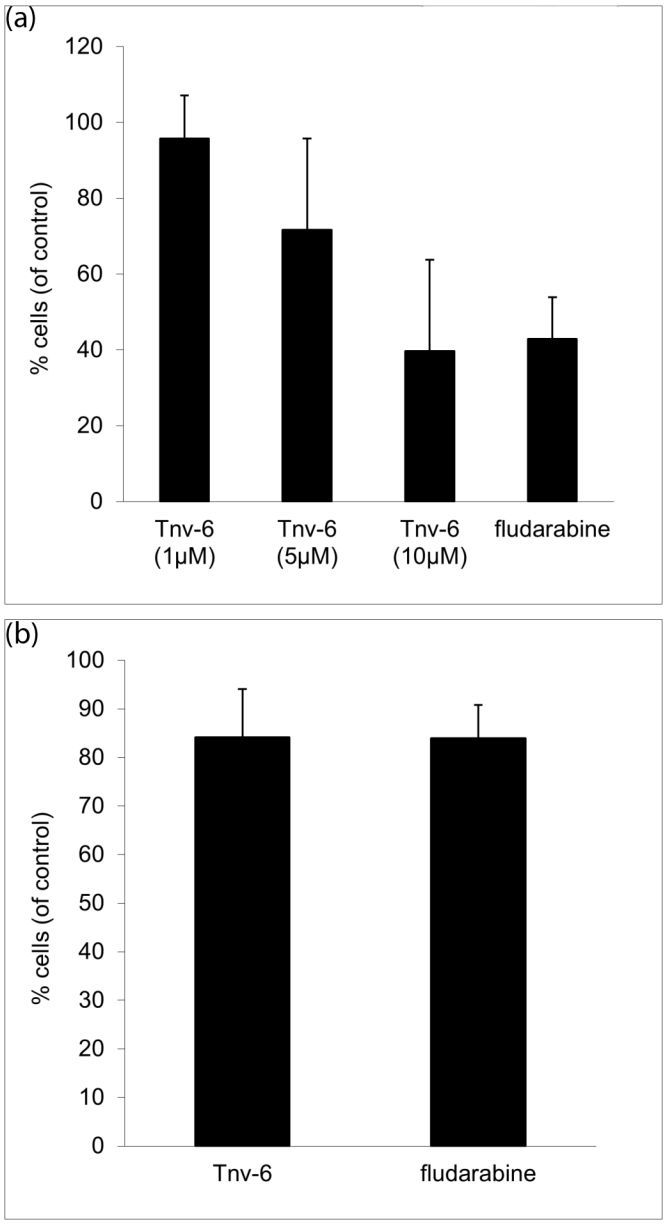


**Figure 1 | Dose-dependent cytotoxicity of Tnv-6.** Compared to 5 μM or 1 μM, greater cytotoxicity to CLL cells was evident with 10 μM of Tnv-6 at 24 hours ($n = 10$, $p = 0.005$, Student's t-test on paired samples), and at equivalent levels to 3 μM fludarabine (a). Cytotoxicity with 10 μM Tnv-6 at 8 hours (relative to controls, $p = 0.007$,) was also similar to fludarabine-containing cultures ($p$ = non-significant) (b).

**Tnv-6 does not induce p53 or apoptosis in CLL.** Intracellular proteins reportedly altered by Tnv-6 treatment in malignant cell lines[23] were investigated in cultured CLL cells (Figure 3 and Supplementary Figure 2). As expected, levels of phosphorylated γ-H2AX were unchanged following exposure to Tnv-6 (0.86 ± 0.17-fold over levels in controls; $p = 0.6$), confirming the drug's non-genotoxic properties[24,25]. Unexpectedly however, no consistent increase in total p53 was detected, with the heterogeneity in expression resulting in no significant overall change (1.5 ± 0.37-fold, $p = 0.37$) over controls. In contrast, induction of p53 was evident in all specimens cultured with fludarabine (3.8 ± 1.7-fold; $p = 0.007$). No consistent up-regulation of p21/waf1 or acetylation of

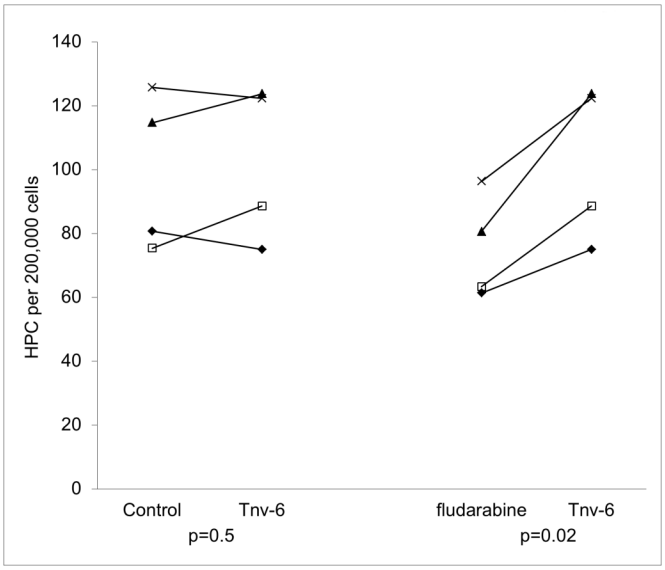


**Figure 2 | Human hematopoietic progenitor cell development (HPC) with Tnv-6.** Numbers of HPC recovered after 8 hours of culture of normal peripheral blood mononuclear cells with control medium (Control), Tnv-6 (10 μM) or fludarabine (3 μM). The recovery of HPC from Controls and cultures incubated with Tnv-6 was equivalent ($p = 0.5$), but higher than in fludarabine-containing cultures ($p < 0.05$, Student's t-test on paired samples), suggesting that the anti-leukemic dose of Tnv-6 is non-toxic to human HPC *in vitro*.

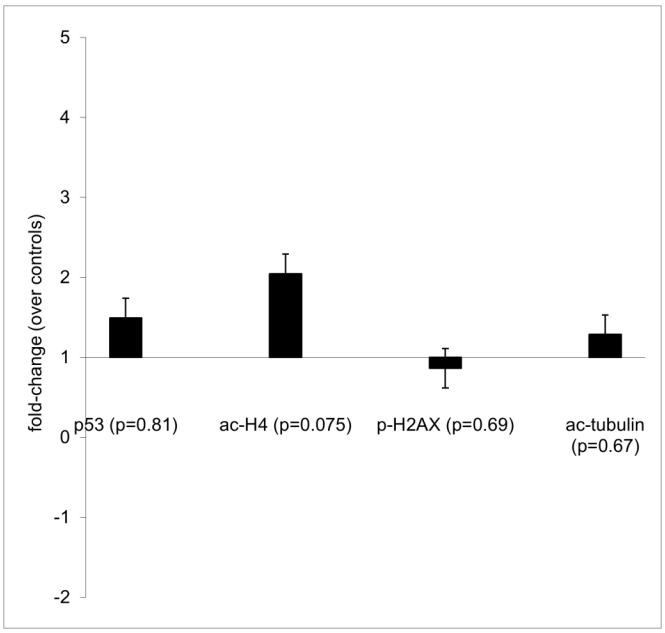


**Figure 3 | Expression levels of select Sirtuin substrates following treatment with Tnv-6.** Levels of p53, acetylated histone H4 (ac-H4), and acetylated tubulin (acet-tubulin) from 8 hour cultures of CLL cells with Tnv-6 were quantified using densitometry, standardized to respective β-actin values and expressed as the fold-change over untreated (control) cultures. In addition, phosphorylated H2AX (p-H2AX) levels were also quantified. Although heterogeneity of p53 and acet-H4 expression existed between patients, no significant difference in levels of any of the proteins was evident in Tnv-6-treated cells (Student's t-test on paired samples).

p53 and tubulin was evident, with variable increases in acetylated Histone-H4 (2.0 ± 0.57-fold; $p = 0.075$). These expression profiles were consistent in repeat cultures with Tnv-6. To exclude the possibility that longer periods of drug-exposure could alter protein expression, CLL cells were cultured with Tnv-6 (at doses of 1, 5 or 10 μM) for 24 hours. However, protein-expression remained unchanged in these extended cultures, and with the use of freshly isolated cells in culture. Interpretation of results from 24 hour cultures with 10 μM Tnv-6 was confounded by variable cell recovery and inconsistent expression of β-actin.

When cells were examined for changes in proteins associated with apoptotic signaling, cleaved PARP-1 and caspase-3 were not detected in any specimen either at 8 or and 24 hours, unlike in fludarabine-treated cultures (Figure 4).

**Tnv-6 induces a distinct transcriptomic profile in CLL.** To identify the mechanisms by which Tnv-6 acts and the comparison with the action of a broad spectrum HDAC inhibitor, we performed global gene expression profiling of cells ($n = 5$) treated with Tnv-6 or TSA as single agents, or with the two HDAC inhibitors simultaneously. Normalization and expression values for arrays were calculated using both dCHIP and RMA with the Affy packages available from Bioconductor[31,32]. Similar results were obtained using dCHIP or RMA, helping to confirm the validity of the expression data obtained. Results are presented only for dCHIP data. After filtering gene sets to remove those that are not expressed, unsupervised hierarchical clustering of the remaining 18,421 gene probe sets identified two distinct clusters of samples, the first representing control samples and cells treated with Tnv-6 and the second cluster consisting of cells treated with either TSA alone or with combination therapy (Tnv-6 and TSA) [Supplementary Figure

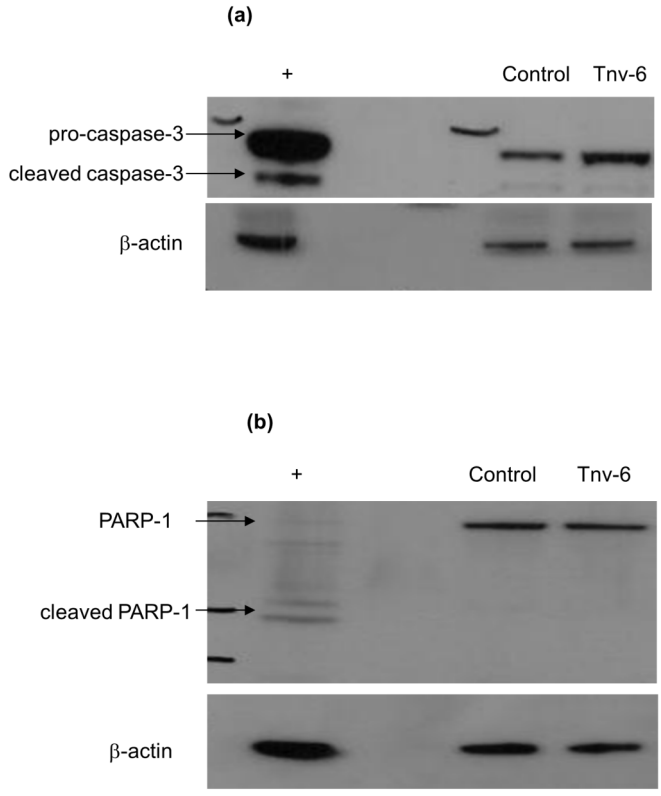


**Figure 4 | Pro-apoptotic protein marker expression following Tnv-6 treatment.** Representative Western blot gel images reveal the absence of cleaved caspase-3 (a) and PARP-1 (b) in CLL cells cultured with Tnv-6 (Tnv-6), similar to untreated cultures (Control). In contrast, cleaved forms of both proteins were detected in CLL cells cultured with fludarabine (+).

3(a)]. In the first cluster there is a clear distinction between the expression profiles of the control samples and those following Tnv-6 treatment, allowing the identification of genes altered by Tnv-6 treatment. Within the second cluster, each of the five patients forms a unique sub-branch, in which the combined treatment consistently leads to an overall gene expression profile that is closer to the Tnv-6 cluster. The clustering pattern also indicates that TSA has an overall larger effect on gene expression changes than Tnv-6 [Supplementary Figure 3(b)], in keeping with the broader spectrum of HDAC inhibition by TSA.

Using a criteria of at least 1.5-fold differently expressed (at 90% confidence) and an absolute difference of at least 100 between comparisons with Benjamini and Hochberg false-discovery correction for multiple testing ($P < 0.05$), 450 probe sets were identified as differentially expressed between Tnv-6-treated and control cultures (Supplementary Table 1A). Using the available Gene Ontology annotations, differentially expressed genes included those regulating immune responses and cellular steroid and lipid metabolism. In particular, significant overrepresentation of genes involved in cholesterol biosynthesis was observed ($p = 0.000037$). Consistent with the lack of p53 protein expression in Tnv-6-treated cells, genes associated with p53 activation were not altered (barring a 2.7-fold up-regulation of *CDKN1A*, $p = 0.028$), with no evidence for the induction of growth arrest or apoptotic pathways. Notably, the activity of genes regulating autophagy-lysosomal pathways[36] was significantly altered in the presence of Tnv-6 (Table 1).

In comparison with Tnv-6, twice as many gene probe sets (944) were identified in TSA-treated cells compared to control cells (Supplementary Table 1B). Cells treated with TSA differentially expressed genes involved in amino acid metabolism and cell-cycle regulation. In combination, Tnv-6 and TSA affected the expression levels of 1364 gene probe sets compared to control cells (Supplementary Table 1C), including gene products regulating biological processes affected individually by the two agents, and additionally, cytoskeletal and organelle proteins. Cholesterol biosynthesis was again the dominant intracellular signaling pathway affected by combined HDAC inhibition.

To validate the data, changes in the activity of select genes important for cholesterol biosynthesis were measured in Tnv-6-treated cells ($n = 5$) using real-time PCR. Consistent with the expression array results, significant increases in activity of 3-hydroxy-3-methyl-glutaryl-CoA reductase (*HMGCR*), Lanosterol synthase *(LSS)* and the transcriptional regulator Sterol Regulatory Element-Binding Protein-2 (SREBP-2) were detected in CLL cells cultured for 8 hours with Tnv-6 (Supplementary Figure 4). By gas chromatography-mass spectrometry, the mean cholesterol content (per $10^6$ cells) was 1.8-fold higher in cells exposed to Tnv-6 for 24 hours than in controls ($p =$ NS; data not shown).

Table 1 | Fold-change in autophagy-lysosomal pathway gene activity in transcriptomic profiles of CLL cells following Tnv-6-treatment ($n = 5$). Negative values reflect down-regulation of gene expression

| Gene | fold change | p value |
|---|---|---|
| aryl hydrocarbon receptor nuclear translocator | 1.58 | 0.038 |
| calnexin | 1.58 | <0.001 |
| calpain 10 | 1.44 | 0.032 |
| chromatin modifying protein 2B | 1.76 | 0.001 |
| cyclin-dependent kinase inhibitor 1A (p21, Cip1) | 2.7 | 0.028 |
| cystatin B (stefin B) | 3.17 | 0.008 |
| cystinosis, nephropathic | 2.15 | 0.004 |
| DnaJ (Hsp40) homolog, subfamily B, member 9 | 1.55 | 0.018 |
| Fas (TNFRSF6)-associated via death domain | −1.63 | 0.033 |
| galactosamine (N-acetyl)-6-sulfate sulfatase | −1.52 | 0.044 |
| hexosaminidase A (alpha polypeptide) | 2.08 | 0.017 |
| inositol hexaphosphate kinase 1 | 1.48 | 0.027 |
| lysosomal-associated membrane protein 1 | 2.54 | <0.001 |
| lysosomal-associated membrane protein 2 | 1.8 | 0.027 |
| Niemann-Pick disease, type C2 | 2.25 | 0.017 |
| optineurin | 2.61 | 0.003 |
| phosphoinositide-3-kinase, class 3 | 1.17 | 0.0248 |
| unc-51-like kinase 3 (C. elegans) | 1.53 | <0.001 |
| upstream transcription factor 2, c-fos interacting | 1.73 | 0.011 |
| vacuolar protein sorting 41 (yeast) | 1.34 | 0.042 |

**Tnv-6 increases autophagosomes in CLL cells.** Since autophagy-lysosomal dysregulation was evident in gene expression profiles of Tnv-6-treated CLL cells, we studied the ultrastructure of cultured cells from 3 available specimens with using transmission electron-microscopy (TEM), to clarify mechanisms of Tnv-6-induced cytotoxicity.

By TEM, no changes in chromatin, cytosolic or membrane structure to indicate apoptosis[37] were evident in any of the 3 specimens at 8 or 24 hours following Tnv-6 treatment (Figure 5). In particular, there was no chromatin or cytoplasmic condensation, and nuclear fragmentation and apoptotic bodies were absent. Instead, cells from cultures with Tnv-6 had an increase in double-membrane bound vacuoles within the cytoplasm (Figure 5). These vacuoles contained cellular debris and recognizable cytoplasmic organelles, suggesting they are autophagic in nature[38,39]. We counted these autophagosomal structures in a total of 100 cell-sections from cultures treated with Tnv-6 for 8 hours and controls, and expressed the results as the average number of autophagosomes per cell. A mean 5-fold increase (range 4–6) in numbers of autophagosomes per cell was evident in the presence of Tnv-6 over corresponding controls (Figure 5; $n = 3$; $p = 0.04$), suggesting altered cellular autophagy[38,39] following Tnv-6-treatment.

**Tnv-6 consistently dysregulates autophagy in CLL.** To confirm changes in autophagy in Tnv-6-treated cells, we quantified changes in the key autophagy-pathway cytosolic protein LC3 by Western blotting ($n = 10$)[39,40]. LC3 is small cytosolic ubiquitin-like molecule that is recruited to autophagosomes upon autophagy induction. Here, it is conjugated to lipid, phosphatidylethanolamine, which can readily be visualized by increased mobility in SDS-PAGE and Western blotting. Therefore, an increase in conversion of LC3 (form I) to its lipidated form (LC3-II) occurs during autophagy. We consistently found that Tnv-6 lead to an increase in LC3-II levels ($4.31 \pm 1.1$-fold over controls; $p = 0.01$) [Figure 6 (a)].

Autophagy is a dynamic process that protects cells under metabolic stress conditions, with the early stage formation of autophagosomes being balanced by their degradation upon delivery to lysosomes[40]. Therefore, an increase in autophagosomes and LC3 lipidation, though consistent with autophagy stimulation, could also result from a block in the late stages of autophagy, for example, fusion of autophagosomes with lysosomes[39]. To distinguish between these two possibilities, lysosomal degradation was blocked by treating cultures with 10 nm bafilomycin-A1 (that targets vacuolar-type $H^+$-ATPase), such that stimulation of autophagy following Tnv-6 treatment would result in a synergistic accumulation of LC3-II By analysis of LC3-II bands in Western blot images [Figure 6 (b)] using densitometry, an increased LC3-II expression was evident with bafilomycin-A compared to untreated cells ($p = 0.03$, $n = 3$), similar to the increase in Tnv-6-treated cells. Addition of bafilomycin-A1 to Tnv-6 cultures caused no further increase in LC3-II compared to Tnv-6 only treated samples ($p = 0.15$). This was in contrast to combining bafilomycin-A1 with 4 μM Ku-0063794[41] (known to stimulate autophagy through direct inhibition of the mTOR pathway) in two cultures [Figure 6(c) and Supplementary Figure 5]. These results demonstrate that Tnv-6 does not stimulate autophagy and identify a role for Tnv-6 in the inhibition of the late stages of autophagy.

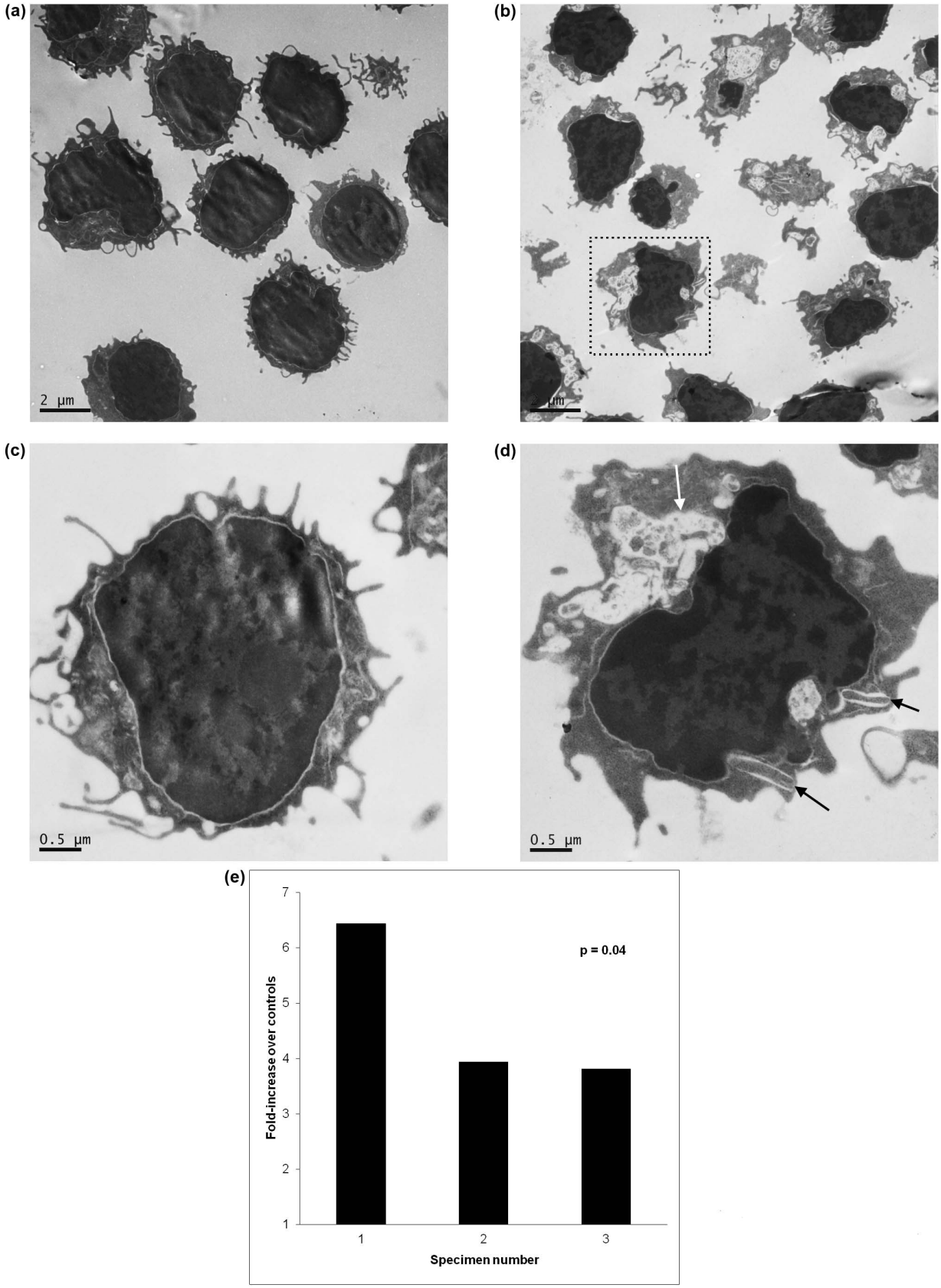


**Figure 5 | Ultrastructural changes following culture with Tnv-6.** Representative TEM images of cells from one (out of 3) CLL specimen after culture without (a) or in the presence of Tnv-6 (b) demonstrate differences in cellular ultrastructure and integrity after Tnv-6 treatment. To visualize subcellular differences in greater detail, images at higher magnification are shown of a cell each from control cultures (c) and Tnv-6 containing cultures (d). The latter cell, highlighted within an interrupted line box in (b) contains double-membrane bound cytoplasmic vacuoles (black arrows) suggestive of early autophagosomes. In addition, larger vacuoles containing morphologically intact material and partially degraded organelles (white arrow) suggestive of late autophagosomes are also seen. Numbers of autophagosomes per cell in 100 cell-sections per culture (n = 3) were 5-fold higher (p = 0.04) in Tnv-6-treated cultures than in corresponding controls (e).

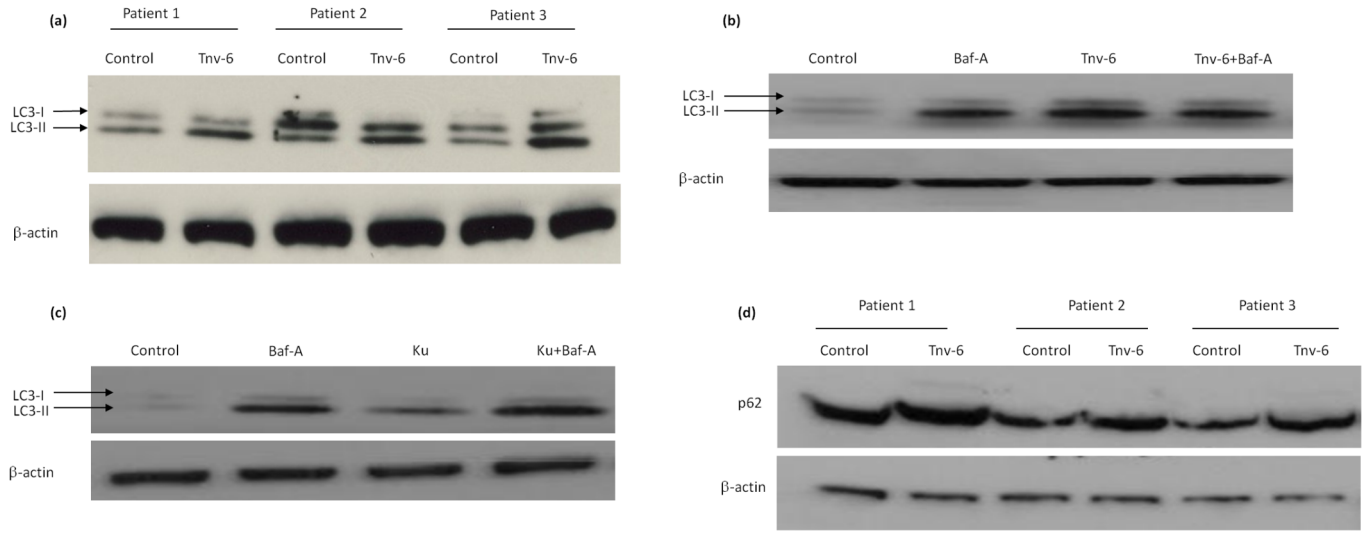


**Figure 6 | Autophagy protein expression profiles following Tnv-6 treatment.** Compared to untreated (Control) cultures, Tnv-6-containing CLL cell cultures had increased lipidated LC3 (LC3-II, indicated by the lower band and arrow) (a). While a similar change in LC3-II was present in cells treated with bafilomycin-A (Baf-A), a synergistic increase in LC3-II was absent when Tnv-6 was combined with bafilomycin-A1 (b), in contrast to cultures with Ku-0063794 and bafilomycin-A1 (c). These data indicating a role for Tnv-6 as an autophagy-inhibitor are supported by the increase in cargo adaptor p62/Sequestosome following Tnv-6 treatment (d).

In support of these data, Tnv-6 treatment resulted in a 1.5-fold increase (range 1.3–1.8) in levels of another autophagy-associated protein p62/SQSTM1 over control cells [n = 3, p = 0.045; Figure 6(d)]. p62 is an LC3 adaptor protein that is degraded by autophagy[40,42], hence an increase in autophagic flux should result in reduced p62 levels[43]. As the opposite in seen with Tnv-6, this indicates, along with the increased number of autophagosomes seen by TEM and the block in LC3-II flux, that Tnv-6 inhibits autophagosomal turnover in CLL cells to prevent the protective effect of autophagic recycling of cytoplasmic contents.

## Discussion

Our studies have identified that in CLL cells, the cytotoxic effects of Tnv-6 may occur through the dysregulation of autophagy rather than induction of apoptosis. Since no 'hot-spot' mutations in the DNA-binding domain of *TP53* were detected in cells from any patient and p53-pathway responses to fludarabine were preserved, we were expecting Tnv-6 to increase expression of p53-dependent proteins, with resulting apoptosis[15,24–26]. However, no consistent increase in p53 or p53-dependent transcriptional activity was observed following Tnv-6 treatment, and no changes in caspase-3 and PARP-1 proteins, known to regulate apoptosis via p53-dependent or independent mechanisms[44,45] were detected. Furthermore, TEM, considered the gold standard for detecting apoptosis[37] demonstrated the absence of quintessential ultrastructural apoptotic features, even in cells cultured for extended periods with Tnv-6. In contrast, increased autophagic vacuoles were identified in Tnv-6 treated cells. Corresponding increases in lipidated LC3 and p62/sequestosome, together with changes in autophagy-lysosome pathway gene activity provide strong evidence for an altered autophagic-flux in CLL cells cultured with Tnv-6 that occurs in the absence of significant p53 expression. Further evidence for the p53-independent dysregulation of autophagy by Tnv-6 comes from the 2-fold increase in LC3 expression-intensity observed in cells from a patient with del(17p) CLL (commonly associated with mutant *TP53*[5]) following culture with Tnv-6 (Supplementary Figure 6), but these results require confirmation in larger studies.

A role for Tnv-6 in inhibiting autophagy is suggested by the increase in p62/sequestosome[41] and supported by the absence of synergistic accumulation of lipidated LC3 in cells cultured with Tnv-6 and bafilomycin-A1[43]. Since autophagy is a pro-survival cellular strategy to maintain homeostasis[40], inhibiting the protective effect of autophagic recycling of cytoplasmic contents can lead to cell death in CLL cells. The up-regulation of cholesterol synthesis genes in Tnv-6-treated cells could reflect a compensatory response to a block in LDL/cholesterol trafficking within the endocytic system, lysosomal dysfunction and changes in autophagy[36].

Tnv-6′s ability to dysregulate autophagy in the absence of p53 up-regulation in CLL cells contrasts with the p53-dependent apoptosis reported in other neoplastic cells[24–27] and could reflect biological differences between different cell-types. In contrast to the tumor cells examined previously[24–27], most CLL cells are quiescent and metabolically inactive in culture. Whether the cellular response to Tnv-6 is influenced by cell-cycle status or cellular metabolic activity therefore requires investigation. Alternatively, the preferential dysregulation of autophagy in CLL may arise from differences in the relative inhibition of SirT1 and SirT2 by Tnv-6[23,28] compared to other cells. Many studies have firmly established the ability of Tnv-6 to inhibit Sirtuins[24–27,46,47] and the altered activity of Sirtuin-dependent genes regulating metabolism[48] seen here in the transcriptome of cells cultured with Tnv-6 does suggest inhibition of SirT1/SirT2 activity in CLL cells. Furthermore, the Tnv-6 effects would be consistent with its Sirtuin inhibitory properties since a role for SirT1 in promoting autophagy independent of p53 acetylation and activation during the cellular survival response to starvation is recognized[20]. However, the precise potency of Sirtuin inhibitors (including Tnv-6) against SirT1 and SirT2 remains difficult to interpret, making cellular responses dependent on the cell-type or Sirtuin antagonist under investigation. This context-dependent biological behavior could account for the differences in results between studies[15,16,20,24–27]. Correlating levels of SirT1 expression with Tnv-6 cytotoxicity could enable comment on whether Tnv-6′s effects could be mediated through SirT1 inhibition, but the presence of multiple protein bands in some patients and the semi-quantitative nature of densitometry-based measurements is likely to confound an accurate assessment of SirT1 levels in CLL cells. In addition, the expression levels of SirT1 may not be a true reflection of functional activity within cells, since its function can be influenced by post-translational modifications, subcellular localization and interactions with other proteins[49]. Experimental manipulation of cellular SirT1 and/or SirT2 levels in cells towards

phenocopying or antagonizing the effects of Tnv-6 would be an attractive way to directly determine whether relative changes in SirT content can alter the cellular response to Tnv-6, but the biological characteristics of primary human CLL cells make these studies technically challenging.

While the precise signaling involved in the cytotoxicity of Tnv-6 to CLL cells remains to be elucidated, our studies demonstrate clearly that Tnv-6, previously thought to mainly mediate p53-mediated apoptotic responses, can be cytotoxic to CLL cells through a novel mechanism, dysregulated autophagy. We further show that this compound acts to inhibit autophagic-flux rather than initiate the autophagic process, highlighting the importance of autophagy to stress responses in CLL and the potential therapeutic utility of targeted manipulation of autophagic-flux in CLL[50,51].

## Methods

**Cell separation and processing.** All studies were performed following approval from Tayside Committee on Medical Research Ethics and Tayside Tissue Bank and all patents gave informed consent for the use of their tissue for this study. Blood (20 ml) was taken from 10 patients (median age 67 years, range 57–78) with CLL and a total white cell count $> 50 \times 10^9$/l (normal range 4–11), not currently on any treatment. Three patients with stable disease were treatment-naive, 3 previously untreated patients had progressive disease and 4 with stable disease had completed therapy at least 12 months prior to the date of blood sampling. Enriched populations of CLL cells were isolated by density gradient centrifugation (Ficoll-Paque™ Plus, 1.077, GE Healthcare Bio-Sciences AS, Uppsala). The enrichment for neoplastic cells (> 92%) was confirmed by the co-expression of CD5 and CD19 by flow-cytometry (FACSscan). Genomic DNA was extracted from CLL cells using the Qiagen BioRobot EZ1 (Qiagen) using protocols (EZ1 DNA Blood Card) recommended by the manufacturer (Qiagen). Samples were quantified by spectrophotomeric reading using the NanoDrop® ND-1000 (NanoDrop Technologies) and stored at −80°C. In addition, cells were cyropreserved in dimethylsulphoxide (Sigma, Steinheim, Germany) in Tayside Tissue Bank for use in cell culture studies. Previous studies[1,29] have suggested the concordance of gene and protein expression in fresh and cryopreserved CLL cells from individual patients, nevertheless, we validated important observations in freshly isolated CLL cells.

***TP53* sequence analysis.** Exons 5–9 of the *TP53* gene (the mutation hotspot region coding for the DNA binding pf p53) were amplified by PCR using genomic DNA extracted from freshly isolated cells. The purified products were directly sequenced using the ABI PRISM® BigDye™ Terminators V 3.0 sequencing kit and run on an ABI 3130 genetic analyzer (Applied Biosystems).

**Cell culture.** Cryopreserved CLL cells were thawed and washed. Trypan Blue exclusion assays indicated that > 99% of cells were viable prior to culture. Cells were cultured at a final concentration of $2 \times 10^6$ cells/ml in medium (RPMI, Sigma) containing 10% fetal calf serum (Harlan sera-Lab Ltd, Loughborough, UK) at 37°C. Cultured CLL cells were incubated with either 1, 5 or 10 μM Tnv-6, 9-μ-D-arabinosyl-2-fluoroadenine (fludarabine) monophosphate (final concentration of 3 μM, Sigma), or Trichostatin-A (TSA) (Sigma, 40 nM) that inhibits Class I, II and IV HDAC. The synthesis of Tnv-6 including full analytical characterization has been described recently[23]. Cultures containing fludarabine served as 'positive' controls to compare the effects of Tnv-6. 'Negative' controls consisted of cultures containing an appropriate volume of drug diluent.

**Cytotoxicity assay.** The CellTiter 96 Aqueous One Solution Assay (Promega) was used to screen for the effects of Tnv-6 on CLL cells. The results enabled identification of incubation times and Tnv-6 doses for a detailed characterization of the biological responses to Tnv-6.

**Expression of intracellular proteins.** Intracellular protein expression following Tnv-6 treatment was studied by Western blot analysis of cultured CLL cell lysates. In brief, cells were lysed on ice using buffer containing 1%Tergitol-type NP-40, 0.5% sodium deoxycholate, 0.1% SDS, protease and phosphatase inhibitors, and snap-frozen and thawed three times. Following centrifugation at 14,000 rpm for 10 minutes at 4°C, protein concentration was determined by Pierce Bicinchoninic Acid (BCA) assay and samples stored at −80°C. Equal amounts of proteins for each sample were migrated in 10% SDS-PAGE, blotted onto nitrocellulose filters, blocked with a 10% suspension of dried skimmed milk in PBS, and incubated with antibodies to SirT1 (1 : 1000, Upstate 07-131), total p53, (DO1, 1 : 100) and p21/waf1 (clone 118, 1 : 1000), kindly gifted by Dr B Vojtesek, Masaryk Memorial Cancer Institute, Brno, Czech Republic), acetylated p53 (Ac-p53 K373-382, Upstate1 : 250), acetylated Histone H4 (Sigma, 1 : 200), acetylated tubulin (Sigma, 1 : 1000), cleaved caspase-3 (Cell Signaling, 1 : 1000), cleaved poly (ADP-ribose) polymerase (PARP-1 Santa Cruz,1 : 500), phosphorylated γ-H2AX (Cell Signaling, 1 : 500), microtubule-associated protein 1 light chain 3 (LC3, Sigma, 1 : 1000) and p62/sequestosome (Abnova, 1 : 1000).

As a control for protein loading, the lower part of each membrane was re-probed with a mouse monoclonal antibody to β-actin (AC-74; Sigma). Immunoreactive bands for proteins of interest were quantified by densitometry in a linear range using calibrated office scanner and ImageJ software, and the ratio of the immunoreactive protein bands and β-actin was calculated. Protein levels from cells cultured with Tnv-6 were expressed as the fold-change over control cultures on the same membrane.

**Global gene expression profiling.** Given the relatively restricted effects of Tnv-6 against HDAC[24,25], we investigated whether Tnv-6-treatment altered a different gene program in CLL cells, compared to a more broad-spectrum HDAC inhibitor such as TSA. Global gene expression profiling of cells treated with Tnv-6 or TSA as single agents, or treated with the two HDAC inhibitors simultaneously was therefore performed. In brief, RNA was extracted from cells following culture with Tnv-6, TSA or a combination of the two agents, and control cultures using the RNeasy® Mini Kit (Qiagen). After reverse transcription, synthesis of biotinylated cRNA and fragmentation of labeled cRNA, probes were hybridized to Affymetrix GeneChip® Human U133 Genome 2.0 arrays (BioScience, Nottingham, UK) at the MRC geneservice (Cambridge, United Kingdom), capable of analyzing the relative expression level of greater than 47,000 transcripts and variants, including more than 38,500 well-characterized genes and UniGenes. All specimens passed standard RNA quality and cDNA/cRNA efficiency tests before being hybridized and all arrays passed the recommended quality control assessments performed in BioConductor and Dchip[30–32]. Percentages of probe sets where the mean signal of the mismatch probes (MM) was greater than the corresponding perfect match (PM) were calculated along with RNA degradation plots using AffyRNAdeg. Images of all Chips were inspected for defects. We also used the in-built outlier detection methods in dCHIP together with percentage present calls, analysis of box-plots and histograms and the RNAdeg packages available on BioConductor as recommended for quality control prior to analysis of data. All arrays performed above the recommendations.

Raw data on global gene expression profiles were uploaded in dCHIP (version 3.7.0) for normalization and supervised and unsupervised analysis[30]. Genes were filtered to remove probes that are not changed across conditions (coefficient of variation 0.2 < SE/mean < 1,000), and to include only those probe sets that are called "present" in at least one condition, have low variation between replicates [0 < median (SD/mean) < 0.5], and have an expression value > 50 in at least one set of replicate samples. Genes were selected at significance ($P < 0.05$ with false discovery rate correction) and a mean fold-difference (at least 1.5-fold at 90% confidence) between the 2 groups for Bayesian classification. Supervised analysis was used to identify genes and pathways/signatures associated with specific drug treatments. MIAME-compliant microarray data will be deposited in NCBI's Gene Expression Omnibus.

**Electron microscopy.** Sub-cellular changes in CLL cells following exposure to Tnv-6 were studied by fixing cultured cells in 4% PFA, 2.5% gluteraldehyde in 0.2 M PIPES. Cells were post-fixed in 1% osmium tetroxide, washed in $dH_2O$, dehydrated through graded ethanols into propylene oxide and then infiltrated with Durcupan resin through propylene oxide/Durcupan steps. Tissue in Durcupan was then placed in moulds and baked at 60°C overnight. Thin sections (Leica Ultramicrotome) were stained with uranyl acetate and lead citrate[33], semi-thin and ultra-thin sections were stained with Richardson's stain (1% toluidine blue and 1% methylene blue in 1% borax) and viewed on a TECNAI 12 (FEI) transmission electron microscope.

**Effects of Tnv-6 on human hematopoietic progenitor development *in vitro*.** The potential hematopoietic toxicity of Tnv-6 was studied in suspension cultures of human hematopoietic progenitor cells (HPC). Briefly, $2 \times 10^6$ blood cryopreserved MNC from healthy volunteers were washed and incubated in 10% fetal calf serum and Iscove's Modified Dulbecco's Medium at 37°C with or without Tnv-6 or fludarabine. Following culture, cells were recovered and washed. A total of $2 \times 10^5$ cells were assayed for erythroid (BFU-E) and myeloid (CFU-GM) HPC in semi-solid clonogenic medium (STEMCELL Technologies, Vancouver, Canada), in accordance to the manufacturer's instructions. The sum total of BFU-E and CFU-GM in $2 \times 10^5$ cultured MNC was used to measure changes in HPC following exposure to Tnv-6 or fludarabine.

**Effects of Tenovin-6 on murine hematopoiesis.** Tnv-6 at a dose of 50 mg/kg was administered by intraperitoneal injection to female SCID mice (Harlan) in a schedule shown to delay growth of tumour cells in xenograft models[24]. This dosing schedule was equivalent to an *in vitro* dose of 8.9 μM. The animals were sacrificed at 7 and 19 days. Cell numbers in blood, bone marrow and spleen were assessed morphologically after staining with Hematoxylin and Eosin and compared with control animals not exposed to Tnv-6.

**Statistical analysis.** The arithmetic mean was used to measure the central tendency of data and the dispersion of values around the mean was expressed as the standard deviation (s.d.) in analysis of raw data, i.e. mean ± s.d. The significance of difference between mean values was determined using Student's t-test (paired). All p-values were two-tailed and statistical-significance was set at the level of $p < 0.05$.

1. Rosenwald, A. *et al.* Fludarabine treatment of patients with chronic lymphocytic leukemia induces a p53-dependent gene expression response. *Blood.* **104**, 1428–1434 (2004).
2. Moussay, E. *et al.* Determination of genes and microRNAs involved in the resistance to fludarabine in vivo in chronic lymphocytic leukemia. *Mol Cancer.* **9**, 115 (2010).

3. Ferracin, M. *et al*. MicroRNAs involvement in fludarabine refractory chronic lymphocytic leukemia. *Mol Cancer.* **9**, 123 (2010).
4. Pettitt, A. R. *et al*. p53 dysfunction in B-cell chronic lymphocytic leukemia: inactivation of ATM as an alternative to TP53 mutation. *Blood.* **98**, 814–822 (2001).
5. Zenz, T. *et al*. TP53 inactivation is associated with poor prognosis in chronic lymphocytic leukemia: results from a detailed genetic characterization with long-term follow-up. *Blood.* **112**, 3322–3329 (2008).
6. Malcikova, J. *et al*. Monoallelic and biallelic inactivation of TP53 gene in chronic lymphocytic leukemia: selection, impact on survival, and response to DNA damage. *Blood.* **114**, 5307–5314 (2009).
7. Zenz, T. *et al*. Detailed analysis of p53 pathway defects in fludarabine-refractory chronic lymphocytic leukemia (CLL): dissecting the contribution of 17p deletion, TP53 mutation, p53–p21 dysfunction, and miR34a in a prospective clinical trial. *Blood.* **114**, 2589–2597 (2009).
8. Hallek, M. *et al*. Addition of rituximab to fludarabine and cyclophosphamide in patients with chronic lymphocytic leukaemia: a randomised, open-label, phase 3 trial. *Lancet.* **376**, 1164–1174 (2010).
9. Inoue, S., Mai, A., Dyer, M. J. & Cohen, G. M. Inhibition of histone deacetylase class I but not class II is critical for the sensitization of leukemic cells to tumor necrosis factor-related apoptosis-inducing ligand-induced apoptosis. *Cancer Res.* **66**, 6785–6792 (2006).
10. Ellis, L., Atadja, P. W. & Johnstone, R. W. Epigenetics in cancer: targeting chromatin modifications. *Mol Cancer Ther.* **8**, 1409–1420 (2009).
11. Lane, A. A. & Chabner, B. A. Histone deacetylase inhibitors in cancer therapy. *J Clin Oncol.* **27**, 5459–5468 (2009).
12. Bots, M. & Johnstone, R. W. Rational combinations using HDAC inhibitors. *Clin Cancer Res.* **15**, 3970–3977 (2009).
13. Stamatopoulos, B. *et al*. Antileukemic activity of valproic acid in chronic lymphocytic leukemia B cells defined by microarray analysis. *Leukemia.* **23**, 2281–2289 (2009).
14. El-Khoury, V. *et al*. The histone deacetylase inhibitor MGCD0103 induces apoptosis in B-cell chronic lymphocytic leukemia cells through a mitochondria-mediated caspase activation cascade. *Mol Cancer Ther.* **9**, 1349–1360 (2010).
15. Audrito, V. *et al*. Nicotinamide blocks proliferation and induces apoptosis of chronic lymphocytic leukemia cells through activation of the p53/miR-34a/SIRT1 Tumor Suppressor Network. *Cancer Res.* **71**, 4473–4483 (2011).
16. Cea, M. *et al*. Synergistic interactions between HDAC and Sirtuin inhibitors in human leukemia Cells. *PloS One.* **6**, e22739. (2011).
17. Dali-Youcef, N. *et al*. Sirtuins: the 'magnificent seven', function, metabolism and longevity. *Ann Med.* **39**, 335–345 (2007).
18. Guarantee, L. & Franklin H. Epstein Lecture: Sirtuins, aging, and medicine. *N Engl J Med.* **364**, 2235–2244 (2011).
19. Madeo, F., Tavernarakis, N. & Kroemer, G. Can autophagy promote longevity? *Nat Cell Biol.* **12**, 842–846 (2010).
20. Morselli, E. *et al*. Caloric restriction and resveratrol promote longevity through the Sirtuin-1-dependent induction of autophagy. *Cell Death Dis.* **1**, e10 (2010).
21. Luo, J. *et al*. Negative control of p53 by Sir2alpha promotes cell survival under stress. *Cell.* **107**, 137–148 (2001).
22. Vaziri, H. *et al*. hSIR2(SIRT1) functions as an NAD-dependentp53 deacetylase. *Cell.* **107**, 149–159 (2001).
23. McCarthy, A. R. *et al*. Synthesis and biological characterisation of sirtuin inhibitors based on the tenovins. *Bioorg Med Chem.* **20**, 1779–1793 (2012).
24. Lain, S. *et al*. Discovery, in vivo activity, and mechanism of action of a small-molecule p53 activator. *Cancer Cell.* **13**, 454–463 (2008).
25. McCarthy, A. R., Hollick, J. J. & Westwood, N. J. The discovery of nongenotoxic activators of p53: building on a cell-based high-throughput screen. *Semin Cancer Biol.* **20**, 40–45 (2010).
26. Li, L. *et al*. Activation of p53 by SIRT1 Inhibition Enhances Elimination of CML Leukemia Stem Cells in Combination with Imatinib. *Cancer Cell.* **21**, 266–281 (2012).
27. Yuan, H. *et al*. Activation of stress response gene SIRT1 by BCR-ABL promotes leukemogenesis. *Blood* **119**, 1904–1914 (2012).
28. Sanders, B. D., Jackson, B. & Marmorstein, R. Structural basis for sirtuin function: what we know and what we don't. *Biochim Biophys Acta.* **1804**, 1604–1616 (2010).
29. Orchard, J. A. *et al*. ZAP-70 expression and prognosis in chronic lymphocytic leukaemia. *Lancet.* **363**, 105–111 (2004).
30. Li, C. & Wong, W. H. Model-based analysis of oligonucleotide arrays: expression index computation and outlier detection. *Proc Natl Acad Sci USA.* **98**, 31–36 (2001).
31. Gautier, L., Cope, L., Bolstad, B. M. & Irizarry, R. A. affy--analysis of Affymetrix GeneChip data at the probe level. *Bioinformatics.* **20**, 307–315 (2004).
32. Tumor Analysis Best Practices Working Group. Expression profiling—best practices for data generation and interpretation in clinical trials. *Nat Rev Genet.* **5**, 29–37 (2004).
33. Reynolds, E. S. The use of lead citrate at high pH as an electron-opaque stain in electron microscopy. *J Cell Biol.* **17**, 208–212 (1963).
34. Wang, J. C. *et al*. Histone deacetylase in chronic lymphocytic leukemia. *Oncology.* **81**, 325–329 (2011).
35. Van Damme, M. *et al*. HDAC isoenzyme expression is deregulated in chronic lymphocytic leukemia B-cells and has a complex prognostic significance. *Epigenetics.* Oct 29, **7**, (2012) [Epub ahead of print].
36. Jegga, A. G., Schneider, L., Ouyang, X. & Zhang, J. Systems biology of the autophagy-lysosomal pathway. *Autophagy.* **7**, 477–489 (2011).
37. Taatjes, D. J., Sobel, B. E. & Budd, R. C. Morphological and cytochemical determination of cell death by apoptosis. *Histochem Cell Biol.* **129**, 33–43 (2008).
38. Eskelinen, E. L., Reggiori, F., Baba, M., Kovács, A. L. & Seglen, P. O. Seeing is believing: the impact of electron microscopy on autophagy research. *Autophagy.* **7**, 935–956 (2011).
39. Barth, S., Glick, D. & Macleod, K. F. Autophagy: assays and artifacts. *J Pathol.* **221,** 117–1124 (2010).
40. Glick, D., Barth, S. & Macleod, K. F. Autophagy: cellular and molecular mechanisms. *J Pathol.* **221**, 3–12 (2010).
41. García-Martínez, J. M. *et al*. Ku-0063794 is a specific inhibitor of the mammalian target of rapamycin (mTOR). *Biochem J.* **421**, 29–42 (2009).
42. Bjørkøy, G. *et al*. p62/SQSTM1 forms protein aggregates degraded by autophagy and has a protective effect on huntingtin-induced cell death. *J Cell Biol.* **171**, 603–614 (2005).
43. Klionsky, D. J. *et al*. Guidelines for the use and interpretation of assays for monitoring autophagy. *Autophagy.* **8**, 445–544 (2012).
44. Kim, R. *et al*. Regulation and interplay of apoptotic and non-apoptotic cell death. *J Pathol.* **208**, 319–26 (2006).
45. Pettitt, A. R., Sherrington, P. D. & Cawley, J. C. Role of poly(ADP-ribosyl)ation in the killing of chronic lymphocytic leukemia cells by purine analogues. *Cancer Res.* **60**, 4187–4193 (2000).
46. Marshall, G. M. *et al*. SIRT1 promotes N-Myc oncogenesis through a positive feedback loop involving the effects of MKP3 and ERK on N-Myc protein stability. *PLoS Genet.* **7**, e1002135 (2011).
47. Wang, B. *et al*. NAMPT overexpression in prostate cancer and its contribution to tumor cell survival and stress response. *Oncogene.* **30**, 907–921 (2011).
48. Walker, A. K. *et al*. Conserved role of SIRT1 orthologs in fasting-dependent inhibition of the lipid/cholesterol regulator SREBP. *Genes Dev.* **24**, 1403–1417 (2010).
49. Houtkooper, R. H., Pirinen, E. & Auwerx, J. Sirtuins as regulators of metabolism and healthspan. *Nat Rev Mol Cell Biol.* **13**, 225–238 (2012).
50. Mahoney, E. *et al*. ER stress and autophagy: new discoveries in the mechanism of action and drug resistance of the cyclin-dependent kinase inhibitor flavopiridol. *Blood.* **120**, 1262–1273 (2012).
51. Kovaleva, V. *et al*. miRNA-130a targets ATG2B and DICER1 to inhibit autophagy and trigger killing of chronic lymphocytic leukemia cells. *Cancer Res.* **72**, 1763–1772 (2012).


## Acknowledgements

We are grateful to TENOVUS Tayside for funding the study. We acknowledge Dr Andrew Cassidy, DNA Sequencing Facility, Ninewells Hospital, Dundee, for support with *TP53* mutational analysis and real-time PCR and Dr Ben Stern, Analytical Centre, University of Bradford, for technical support with gas chromatography-mass spectrometry.

## Author contributions

S.F.M. and M.J.G. performed all cell culture and protein expression studies. J.J. and A.R.P. performed electron microscopy. A.A.D. and A.N. performed gas chromatography-mass spectrometry. J.C. and S.H. performed and interpreted FISH studies. K.M. and V.A. performed animal studies. N.J.W. manufactured Tenovin-6. I.G.G. designed and interpreted autophagy studies. P.J.C. interpreted gene expression studies. S.T., S.L., P.J.C. and I.G.G. designed the study. S.T. drafted the manuscript. All authors reviewed the manuscript.

## Additional information

**Supplementary information** accompanies this paper at http://www.nature.com/scientificreports

**Competing financial interests:** The authors declare no competing financial interests.



**How to cite this article:** MacCallum, S.F. *et al*. Dysregulation of autophagy in chronic lymphocytic leukemia with the small-molecule Sirtuin inhibitor Tenovin-6. *Sci. Rep.* **3**, 1275; DOI:10.1038/srep01275 (2013).